SLAC-PUB--5324

DE91 007415

POSSIBLE EXPERIMENTAL STUDIES OF THE $t\bar{t}$ THRESHOLD REGION AT 250–500 GeV e^+e^- COLLIDER*

Sachio Komamiya

Stanford Linear Accelerator Center, Stanford University, Stanford, CA 94309

ABSTRACT

A possible measurement of the top quark mass by an energy scan of the $t\bar{t}$ threshold region at e^+e^- colliders of $\sqrt{s}$ = 250–500 GeV is discussed. With an integrated luminosity of 1 fb^{-1} devoted to the energy scan, a top quark mass of about 150 GeV can be determined with an accuracy of $\approx$ 0.3 GeV, with a comparable systematic uncertainty arising from the few % errors in the α_s measurement at LEP–I. The possibilities of studying Γ_t and Higgs boson effects are also discussed.

I. INTRODUCTION

If the top quark mass is between 100 GeV and 250 GeV, an e^+e^- collider of $\sqrt{s}$ above LEP–II energies (between 250 GeV to 500 GeV) is an ideal place to study the properties of top quark. In this report a possible measurement of top quark mass and other threshold parameters by energy scan at such a collider is discussed.

The advantage of the energy scan method is that the results do not depend on the details of the detector performance because the measurement is just the cross section for $e^+e^- \rightarrow t\bar{t}$ (number of $t\bar{t}$ events) at each scan point. We assume that the luminosity measurement is sufficiently precise. Even if the background level is not precisely known before the actual energy scan, it can be measured into good precision at an energy point well below the $t\bar{t}$ threshold. The disadvantages are that large integrated luminosity is needed to scan through many points; in addition the machine may need adjustment at each energy point, as we have experienced for the SLC machine. Moreover, if beamstrahlung effects are large so that the beam energy distribution has a long tail in the lower energy side, it might not be easy to measure M_t in a reasonable accuracy by the energy scan. The beamstrahlung correction is very similar to the corrections due to initial state radiation effects. Once the beamstrahlung energy profile is known we can convolute the theoretical cross section with the energy profile. The energy profile can be measured by unfolding the invariant mass distribution of Bhabha events measured at each scan point. To unfold the beamstrahlung energy profile we need a large number of Bhabha events and an excellent energy resolution is required for the EM calorimeter. Also an accurate theoretical Bhabl a cross section with higher order radiative corrections is needed. In this report we neglect the beamstrahlung effects because it is still premature to discuss realistic machine parameters, and because this effect is small in candidate machine designs.

Experimentally, it is highly probable that the top mass will be roughly known from the experiments at Tevatron, LHC or SSC at the time when the e^+e^- collider of $\sqrt{s}$ = 250–500 GeV turns on. At the e^+e^- collider we can measure the top mass from the invariant mass of $W + b$ at a high energy point above the $t\bar{t}$ threshold. The resolution in top quark mass obtained by the invariant mass measurement depends on the energy resolution and the solid angle coverage of the detector. This coarse top mass measurement can be used as an input for a more precise measurement by an energy scan.

The cross section of $t\bar{t}$ near the threshold is sensitive to the strong coupling α_s[2]. We assume that α_s can be determined within a few percent level on the Z resonance at LEP–I. We also assume that theoretical ambiguity in the QCD calculations of the $t\bar{t}$ cross sections is small. Especially, the renormalization scale (Q^2) of α_s used in the formula of $t\bar{t}$ threshold and those for the LEP α_s measurements must have a clear and consistent relation.

At the moment we do not know whether we need to perform an energy scan in order to measure the top mass with an accuracy comparable to the W mass resolution at the LEP–II ($\sigma_{M_W} \approx 0.15$ GeV)[1], because a precise top mass measurement can not further constrain the Standard Model in a fundamental way, since fermion masses in the Standard Model are arbitrary parameters, which can be adjusted to the observed masses. On the other hand, measurements of gauge boson masses constrain the Standard Model tightly. However, if we measure M_t precisely, theorists may have stronger motivation to study the origin of fermion masses, which might be related to the quark mixing angles.

* Work supported by Department of Energy contract DE-AC03-76SF00515.

Contributed to the DPF Summer Study on High Energy Physics, Snowmass, CO, June 25–July 13, 1990.

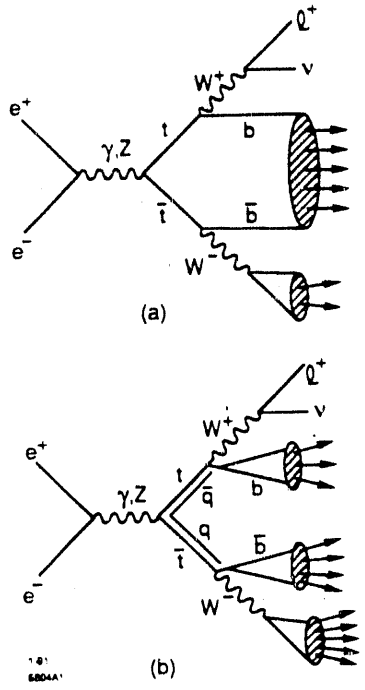

Fig. 1. Schematic diagram to explain the difference of the two hadronization scheme. (a) Top quarks decay into $W+b$ without forming T-hadron. The hadronization takes place in the color singlet system between b and $\bar{b}$, which are decay products of t and $\bar{t}$. (b) Top quarks decay after forming T-hadron. The hadronization takes place in the color singlet system between b [$\bar{b}$] and the spectator anti-quark $\bar{q}$ [spectator quark q].

II. MONTE CARLO SIMULATION

A. *Hadronization of Top Quark*

Since lifetime of a heavy top quark is shorter than the typical time scale of fragmentation [$\approx 1/(200\ \mathrm{MeV})$] in the mass region we are studying[4], the top quark decays before forming a T-hadron (T-meson or T-baryon) and the hadronization occurs between b and $\bar{b}$ as shown in Fig. 1(a). On the contrary, if the top quark mass is light, the top quark forms a T-hadron before its decay, after which the t quark in the T-hadron decays into $b+W$. In this case, the hadronization takes place between b and a spectator quark (or a spectator di-quark) [see Fig. 1(b)]. We studied the following three cases of the hadronization scheme for the process $t\bar{t} \to bW^+\bar{b}W^- \to bf_1\bar{f}_2b\bar{f}_3f_4$:

(a1) Top quark decays into $b+W$ before fragmentation. Decay angular distributions of $t \to b+W$ and $W \to f\bar{f}'$ are assumed to be isotropic. If $b\bar{b}$ invariant mass is larger than 30 GeV, the Lund parton shower model is applied to the $b\bar{b}$ system. Otherwise the Lund string fragmentation is applied to the hadronization of $b\bar{b}$ system.

(a2) Similar to the case (a1) but events are weighted by the correct matrix element squared of the process of $t\bar{t} \to bW^+\bar{b}W^- \to bf_1\bar{f}_2b\bar{f}_3f_4$.†

(b) Top quark is hadronized into T-hadron before its decay. The T-hadron (t plus a spectator) decays into $b+W$ plus a spectator. The color string is stretched between b and the spectator and hadronization occurs along the string as in the Lund model.

For heavy top quarks produced not far from the threshold, the case (a2) is the most realistic simulation. For $\sqrt{s} < 2M_t$, of course, (b) is not valid. The model dependence of the $t\bar{t}$ detection efficiency is investigated and the results are discussed later.

B. *Monte Carlo Generation of Background Events*

The main sources of background events which have relatively large visible energy and charged multiplicity are (1) $e^+e^- \to q\bar{q}$ ($q = d,u,s,c,b$), (2) $e^+e^- \to W^+W^-$ and (3) $e^+e^- \to ZZ$. The Lund shower model[5] is used for the event generator of light quark pairs (including $e^+e^- \to \gamma + Z \to \gamma + q\bar{q}$). The WW and ZZ background are generated by a Monte Carlo of Kleiss et al.[6] in which the spin correlations are taken into account. Gluon emissions in the Z or W hadronic decay is simulated using the Lund shower model[5].

Cross sections for the main background processes assumed for the Monte Carlo studies without and with initial state photon radiative corrections (with the hard photon energy limit is $k_\gamma = 2E_\gamma/\sqrt{s} < 0.99$) are listed in Table I (in units of $\sigma_{\mu\mu}(1st\ order\ QED) = 86.8$ nb/s GeV^2). The $R^{rad}_{q\bar{q}}$ includes the cross section for $e^+e^- \to Z+\gamma \to q\bar{q}+\gamma$. The background cross section is quite high compared to the $t\bar{t}$ cross section, which is about one unit of $\sigma_{\mu\mu}$.

C. *Detector Simulation*

The detector simulation is done in a simple way. The acceptance of the detector is assumed to be perfect except for the region near the beams, and it is assumed that there are no active elements within 10° cones from the beams. The energy and momentum direction of produced stable particles (except for muons) are in principle measured by hadron and electromagnetic calorimeter. To simulate calorimeter in a simple manner, particle pairs with opening angle smaller than 4 degrees are combined into energy clusters. The direction of those energy clusters is smeared with a σ of 2 degrees for each of the two angles corresponding

† The matrix element squared is calculated by M. E. Peskin, assuming massless particles in the final state.

Table I
The R values of various background processes

$\sqrt{s}$	R_{qq}	R_{qq}^{rad}	R_{WW}	R_{WW}^{rad}	R_{ZZ}	R_{ZZ}^{rad}
250 GeV	7.56	29.9	10.4	11.9	0.68	0.78
300 GeV	7.25	28.9	12.2	14.5	0.76	0.90
400 GeV	6.95	28.2	15.4	19.0	0.90	1.11
500 GeV	6.82	28.0	18.1	22.64	1.03	1.30

Table II
The cuts for $t\bar{t}$ event selection (M_t = 150 GeV)

Cut	Cut Definition	$\epsilon_{t\bar{t}}$	ϵ_{qq}	ϵ_{WW}	ϵ_{ZZ}
1	$N_{ch} > 10$	1.000	0.974	0.882	0.893
2	$E_{vis} > 0.4\sqrt{s}$	0.995	0.857	0.871	0.855
3	$\rho_{event} > 3.0$ GeV$^{1/2}$	0.301	0.066	0.304	0.112
4	$M_{\ell} > 130$ GeV	0.247	$<4\ 10^{-5}$	0.0018	0.071
5	$M_{out} > 40$ GeV	0.217	$<4\ 10^{-5}$	0.0088	0.040
6	$M_1 > 90$ GeV or $M_2 > 90$ GeV	0.141	$<4\ 10^{-5}$	0.0022	0.031
7	$\lvert N_1 - N_2\rvert/(N_1 + N_2) > 0.5$	0.124	$<4\ 10^{-5}$	0.0011	0.0079

Table III
The final efficiency of signal and background events

M_t	$\epsilon_{t\bar{t}}$	ϵ_{qq}	ϵ_{WW}	ϵ_{ZZ}
125 GeV	0.169	$<3\ 10^{-5}$	0.0021	0.034
150 GeV	0.124	$<4\ 10^{-5}$	0.0011	0.0079
200 GeV	0.203	$<4\ 10^{-5}$	0.0011	0.0011
250 GeV	0.238	$<4\ 10^{-5}$	0.0009	0.0005

Table IV
Detection efficiency of $t\bar{t}$ events for the three hadronization models

Cut	Cut Definition	$\epsilon_{(a1)}$	$\epsilon_{(a2)}$	$\epsilon_{(b)}$
1	$N_{ch} > 10$	1.000	1.000	1.000
2	$E_{vis} > 0.4\sqrt{s}$	0.998	0.997	0.995
3	$\rho_{event} > 3.0$ GeV$^{1/2}$	0.314	0.303	0.301
4	$M_{\ell} > 130$ GeV	0.277	0.263	0.247
5	$M_{out} > 40$ GeV	0.243	0.241	0.217
6	$M_1 > 90$ GeV or $M_2 > 90$ GeV4	0.193	0.192	0.141
7	$\lvert N_1 - N_2\rvert/(N_1 + N_2) > 0.5$ 4	0.155	0.156	0.124

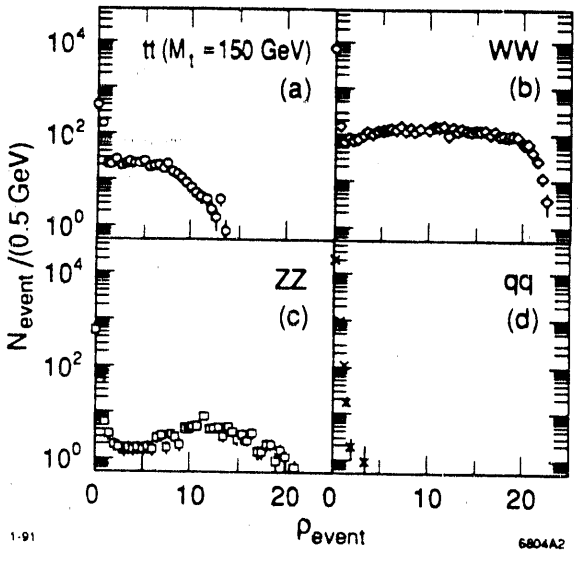

Fig. 2. The distribution of $\rho_{\rm event}$, the maximum value of the lepton isolation parameter ρ_ℓ for all the leptons with $p_\ell > 2$ GeV in an event. The plots are normalized with the same luminosity (also for Figs. 3–6). (a) $t\bar{t}$ events assuming $M_t = 150$ GeV and $R_{t\bar{t}} = 1.0$; (b) W^+W^- events; and (c) ZZ events.

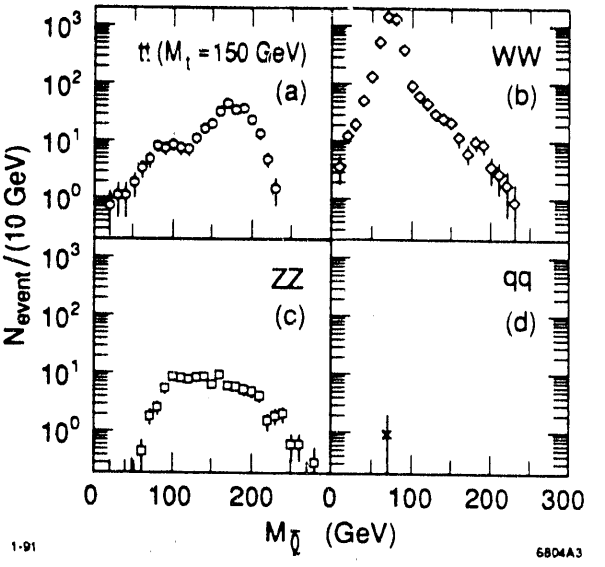

Fig. 3. Invariant mass of all the detected energy clusters except for the most isolated lepton ($M_{\bar{\ell}}$). (a) $t\bar{t}$ events assuming $M_t = 150$ GeV and $R_{t\bar{t}} = 1.0$; (b) W^+W^- events; (c) ZZ events; and (d) $q\bar{q}$ events.

to the two directions perpendicular to the cluster momentum. The energy resolution of the calorimeter is assumed to be $0.50/\sqrt{E\ (\mathrm{GeV})}$ with an offset of 0.020. The electromagnetic calorimeter has an energy resolution of $0.08/\sqrt{E}$ with an offset of 0.005. Lepton identification and background rejection are assumed to be perfect for $p = |\vec{p}| > 2$ GeV. The muon momentum resolution is $\sigma_p/p = 0.0003p$ (p in GeV) for $p > 2$ GeV.

III. EVENT SELECTION

The signatures of top quark events ($e^+e^- \to bW^+\bar{b}W^-$) are isolated leptons from the W leptonic decay and the spherical event shape. Major background processes are $e^+e^- \to W^+W^-$ with one of $W^\pm$ decaying into $\ell\nu$, and $e^+e^- \to ZZ$ with one of Z's decaying into lepton pair and the other decaying hadronically. Light quark pair production (QCD) has large cross section but very few isolated leptons are produced. Since the cross section of $e^+e^- \to ZZ$ is much smaller than for $e^+e^- \to W^+W^-$, we optimized the cuts to efficiently reject W^+W^- events. The following selection criteria are applied.

(1) Number of observed charged particles is greater than 10.

(2) Visible energy (sum of the energy deposited in the electromagnetic and hadron calorimeter plus muon momenta) is greater than $0.4\sqrt{s}$.

(3) The event contains at least one isolated lepton ($e^\pm$ or $\mu^\pm$). The isolation condition is $\rho_\ell > 3.0\ \mathrm{GeV}^{1/2}$, where the isolation parameter ρ_ℓ is defined as follows: The JADE jet-finding algorithm with $y_{cut} = (25\ \mathrm{GeV})^2/s$ is applied[7] to all the energy clusters in the event (except the candidate lepton ℓ). Then

$$\rho_\ell \equiv \min_{jets\ j} \sqrt{2p_\ell(1-\cos\chi_{\ell j})}\quad ,$$

where p_ℓ is the momentum of the lepton and $\chi_{\ell j}$ is the angle between the lepton momentum direction and the reconstructed jet axes. The distribution of $\rho_{\rm event}$, the maximum value of ρ_ℓ over all the leptons in with $p_\ell > 2$ GeV in an event is plotted in Fig. 2(a)–(d).

(4) Invariant mass of all the detected energy clusters except for the most isolated lepton ($M_{\bar{\ell}}$) must be larger than max [130 GeV, 130 GeV $\times$ ($\sqrt{s}$/300 GeV)]. The distribution of $M_{\bar{\ell}}$ after the cut (3) is shown in Fig. 3(a)–(d).

(5) $M_{\rm out}$ is larger than max [40 GeV, 40 GeV $\times$ ($\sqrt{s}$/300 GeV)] where $M_{\rm out} = \sqrt{s}/E_{\rm vis}\sum|p_T^{out}|$. Here, p_T^{out} is transverse momentum of energy clusters measured from the event plane defined by the two major eigenvectors of sphericity analysis. The distribution of $M_{\rm out}$ after the cut (4) is shown in Fig. 4(a)–(c).

(6) The event is divided by two hemispheres perpendicular to the event thrust axis and the in-

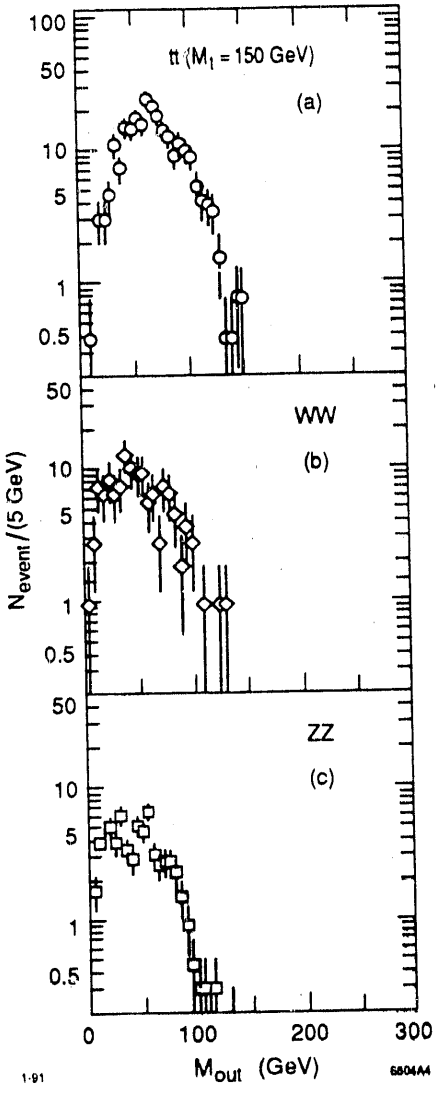

Fig. 4. The distribution of $M_{\rm out}$ after the cut (4). (a) $t\bar{t}$ events assuming $M_t = 150$ GeV and $R_{t\bar{t}} = 1.0$; (b) W^+W^- events; (c) ZZ events; and (d) $q\bar{q}$ events.

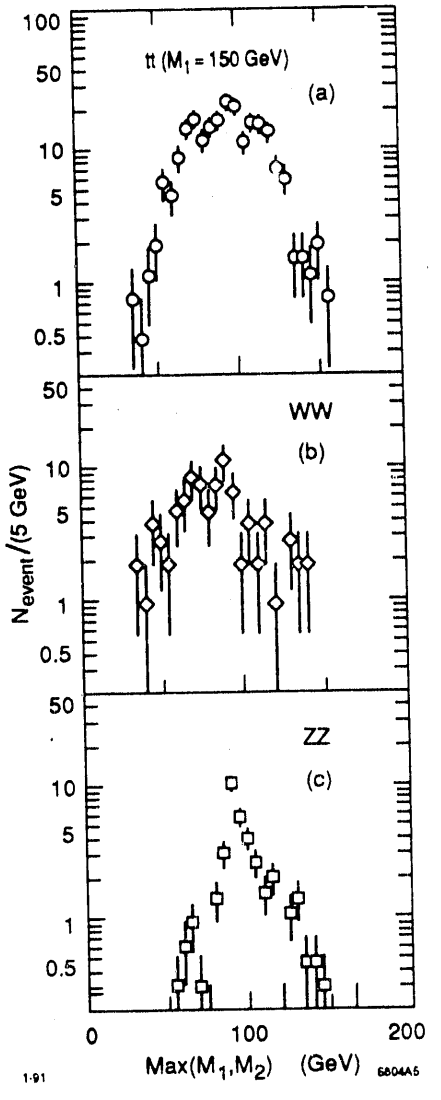

Fig. 5. The distribution of $max(M_1, M_2)$ after the cut (5). (a) $t\bar{t}$ events assuming $M_t = 150$ GeV and $R_{t\bar{t}} = 1.0$; (b) W^+W^- events; and (c) ZZ events.

variant mass of one of the hemispheres (M_1 or M_2) is required to be larger than max [90 GeV, 90 GeV $\times(\sqrt{s}/300$ GeV)]. The distribution of $max(M_1, M_2)$ after the cut (5) is shown in Fig. 5(a)–(c).

(7) Charged multiplicities of the two thrust hemispheres (N_1 and N_2) must satisfy $|N_1 - N_2|/(N_1 + N_2) < 0.5$. The distribution of $|N_1 - N_2|/(N_1 + N_2)$ after the cut (6) is shown in Fig. 6(a)–(c).

The fraction of events surviving after each step of the selection criteria is listed in Table II for $\sqrt{s} =$ 300 GeV and $M_t = 150$ GeV. In the table, numbers are given for $e^+e^- \to t\bar{t}$ as well as for background processes (W^+W^- events ZZ events and $q\bar{q}$ events, where $q = d, u, s, c, b$). For $\sqrt{s} \leq 250$ GeV, the last two cuts [(6) and (7)] are not applied in the event selection in order to have a larger detection efficiency for $t\bar{t}$ events. Detection efficiencies after the cuts, at $\sqrt{s} =$ 250 GeV, 300 GeV, 400 GeV, are listed in Table III for $e^+e^- \to t\bar{t}$ as well as for background processes.

The $t\bar{t}$ detection efficiency does not have a large hadronization model dependence; this is made clean in Table IV. In the table, the efficiencies are compared at $M_t = 150$ GeV for the models (a1), (a2) and (b), which are already described in Sec. II.

The fraction of events with isolated leptons over all $t\bar{t}$ events is at most $\approx 40\%$ including $W \to \tau\nu$: The rest ($\approx 60\%$) are purely hadronic decays. We have not studied the case in which both W's from top

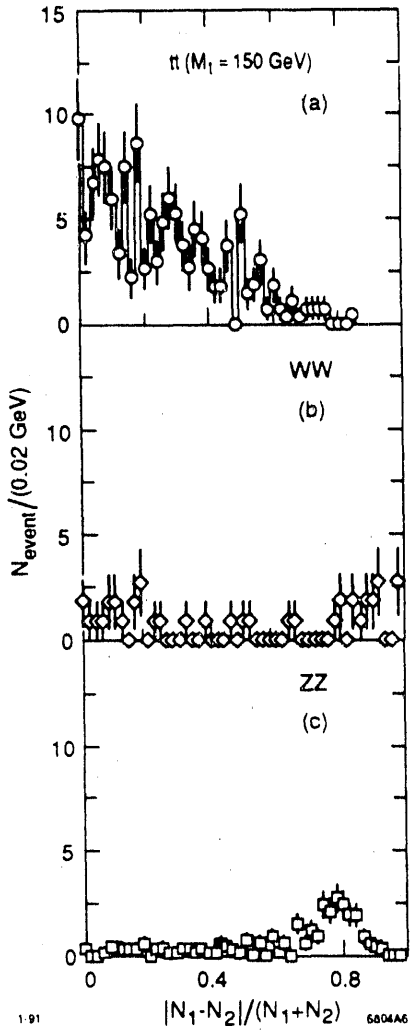

Fig. 6. The distribution of $|N_1 - N_2|/(N_1 + N_2)$ after the cut (6). (a) $t\bar{t}$ events assuming $M_t = 150$ GeV and $R_{t\bar{t}} = 1.0$; (b) W^+W^- events; and (c) ZZ events.

quarks decay hadronically. If M_t is large so that *b-jets* are enough energetic and they are well separated from the jets in the W decay, the event will have several energy-momentum constraints among jets. Therefore it might be possible to reconstruct these events[8]. The b-tagging (by selecting events containing many tracks with large impact parameter) might help to select $t\bar{t}$ events. For lower top masses, however, *b-jets* are soft and many jets coming from W decays are more energetic than the *b-jets*.

IV. ENERGY SCAN

The most efficient way to search for new particles and to look for obvious anomalies against the Standard Model is to sit at the highest energy point where reasonably high luminosity can be also provided. Therefore we assume that M_t is already measured with an accuracy of 5–10%, sitting at the high energy point.

In this report, the study of the energy scan strategy and the calculation of expected errors in the threshold parameters are essentially based on the paper by Swartz[1].

The first crude scan can be started from 20 GeV above the best guess point and scan down the energy with 5 GeV interval (in $\sqrt{s}$) and with the integrated luminosity of 0.1 fb^{-1} per scan point until the $t\bar{t}$ cross section decreases significantly. In the worst case we may have to measure 7 points until the cross section decreases significantly. One more point is added at 5 GeV below the last scan point.

According to Ref. 1, a sensitivity function for M_t

$$S(\sqrt{s}; M_t) = \frac{1}{\sqrt{\sigma_{t\bar{t}}}} \frac{\partial \sigma_{t\bar{t}}}{\partial M_t}$$

is calculated as a function of $\sqrt{s}$. In Fig. 7, $S(\sqrt{s}; M_t)$ is plotted for $M_t = 150$ GeV as well as sensitivity functions of other parameters.

An example of the scan is plotted in Fig. 8. The expected one sigma resolution of M_t is calculated by the formula

$$\Delta(M_t) = \frac{1}{\sqrt{\sum_{i=1}^{N} L_i S(\sqrt{s_i}; M_t)^2}} \quad ,$$

where L_i is integrated luminosity at each scan point. After the first coarse scan, the expected resolution is between 0.3 GeV to 1.2 GeV depending on the initial scan point. This ΔM_t does not include any systematic ambiguities from other parameters. A relatively good ΔM_t of 0.3 GeV can be obtained if one of the scan points is in the sensitive region where $|S(\sqrt{s}; M_t)|$ is large. After this scan we know the M_t with an accuracy of $\approx$ 1 GeV. We choose the case with the worst M_t resolution of 1.2 GeV (8 point scan between 290 and 325 GeV in 5 GeV step). To improve the resolution, two points with 1 GeV interval are added to the most sensitive region calculated from the first scan. For the above example we add two points at 293 GeV and at 294 GeV with 0.1 fb^{-1} for each. The expected M_t resolution decreases from 1.2 GeV to 0.33 GeV. We obtained the relative M_t resolution as good as W mass measurement at LEP-II ($\sigma_{M_W}/M_W = 0.2\%$)[1] with relatively small luminosity.

V. DETERMINATION OF OTHER PARAMETERS

In principle $\sigma_{t\bar{t}}$ is a function of six parameters ($\sqrt{s}$, M_t, Γ_t, α_s, M_H, f_{ttH}), where f_{ttH} is the rela-

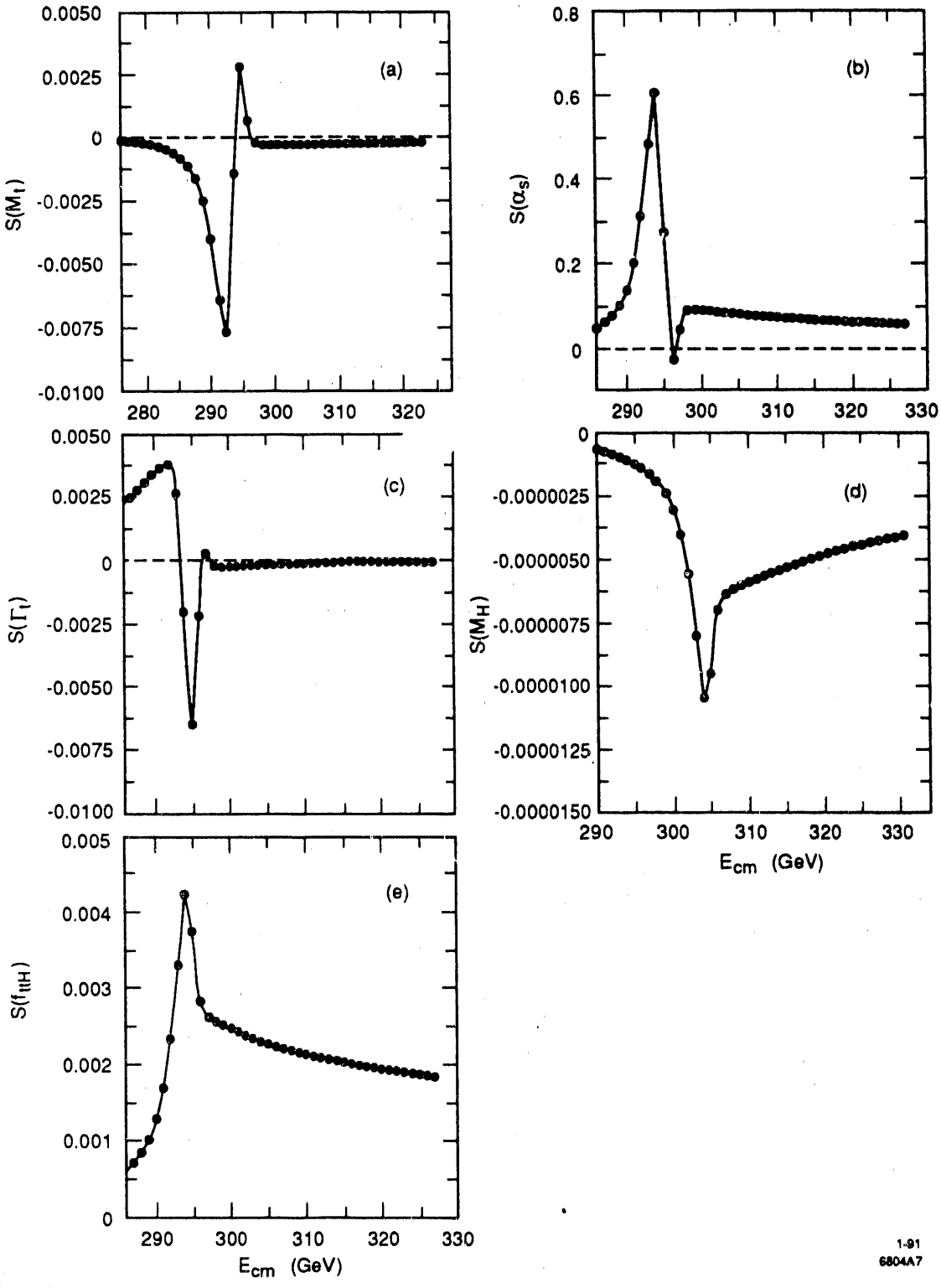

Fig. 7. Sensitivity function defined as $S(\sqrt{s};\alpha_\nu) = (1/\sqrt{\sigma_{t\bar{t}}})(\partial\sigma_{t\bar{t}}/\partial\alpha_\nu)$ for $M_t = 150$ GeV, where α_ν is one of threshold parameters. (a) $\alpha_\nu = M_t$; (b) $\alpha_\nu = \alpha_s$; (c) $\alpha_\nu = \Gamma_t$; (d) $\alpha_\nu = M_H$; and (e) $\alpha_\nu = f_{ttH}$.

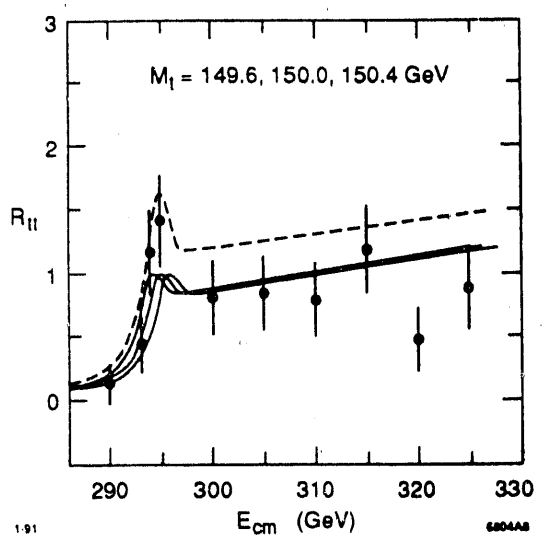

Fig. 8. An example of the energy scan near $t\bar{t}$ threshold. A coarse scan is done with 5 GeV step for 8 points (luminosity of each point is 0.1 fb^{-1}). After the coarse scan, two more points are added in the sensitive region of M_t. The total integrated luminosity is 1 fb^{-1} (0.1 fb^{-1} for each point).

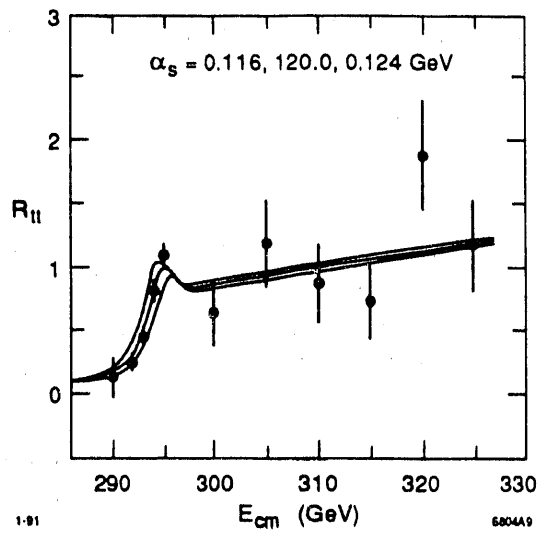

Fig. 9. In addition to the scan as shown in Fig. 8, more luminosity and energy points are added to determine M_t and α_s simultaneously. The total integrated luminosity is 5 fb^{-1}.

tive strength of the coupling constant for the ttH vertex. In the Standard Model, Γ_t and f_{ttH} are not independent parameters because they can be calculated from other parameters. This section discusses the estimation of systematic errors in M_t which come from uncertainties in other parameters, and possibilities of determining these other parameters.

A. The Strong Coupling (α_s)

The most sensitive and unknown uncertainty is in α_s. Roughly speaking, an error $\Delta\alpha_s$ of 0.01 corresponds to ΔM_t of 1 GeV for $M_t = 150$ GeV. If we can measure α_s to 3–5 percent accuracy at LEP–I on the Z resonance, the systematic error of M_t due to the uncertainty in α_s is approximately 0.3–0.5 GeV. However, this value does not include any theoretical uncertainty in the choice of the Q^2 for the $t\bar{t}$ bound state and that for $Q^2 = M_Z^2$. In principle, the relation between the α_s determined at Z resonance (from a differential jet rate[10], for example) and α_s at the $t\bar{t}$ threshold with the same renormalization scheme ($\overline{MS}$), but the complete next-to-the-leading order corrections to the $t\bar{t}$ cross section is not yet calculated and they are expected to be not small (10–20%)[9]. Hopefully, this calculation will be done before the experiments begin.

We also study the possibility to determine M_t and $\alpha_s(Q^2 = M_Z^2)$ simultaneously with larger luminosity. To the previous example of the energy scan (see Fig. 8), we add integrated luminosity of 1.0 fb^{-1} (per point) at the energy points of $\sqrt{s}$ = 292 GeV, 293 GeV, 294 GeV, and 295 GeV at the sensitive region of α_s (as shown in Fig. 9) With the simultaneous fit of M_t and α_s, we expect $\Delta M_t = 0.611$ GeV and $\Delta\alpha_s = 0.0071$. With total luminosity of 5 fb^{-1} we cannot determine α_s better than at LEP–I.

B. Top Decay Width (Γ_t)

The top decay width can be known relatively precisely for a given mass, if we assume $|V_{tb}| = 1.0$ and the Standard Model. However, it would be wonderful to determine this width experimentally. The simplest scanning strategy discussed above leads to an expected one sigma error on the width measurement of 0.383 GeV from a two parameter fit (M_t and Γ_t). The expected mass resolution in the same scan is 0.318 GeV for $M_t = 300$ GeV. There is very small statistical correlation between Γ_t and M_t. Since the expected width for 150 GeV top quark is 0.885 GeV, the width measurement is relatively poor.

The measurement can be improved by adding additional luminosity in the sensitive region 10 points, from 287 GeV to 296 GeV, 1 GeV step with 0.4 fb^{-1} per point in the example of the 150 GeV top mass determination as shown in Fig. 10. For a simultaneous fit of M_t and Γ_t we expect $\Delta M_t = 0.145$ GeV and $\Delta\Gamma_t = 0.176$ GeV assuming other parameters are known to good accuracy.

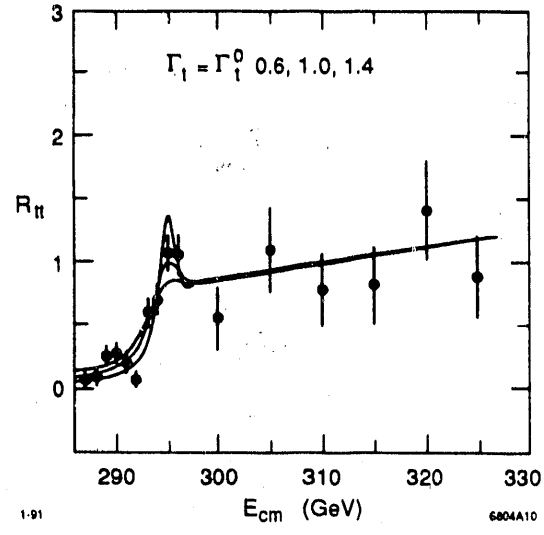

Fig. 10. In addition to the scan as shown in Fig. 8, more luminosity and energy points are added to determine M_t and Γ_t simultaneously. The total integrated luminosity is 5 fb^{-1}.

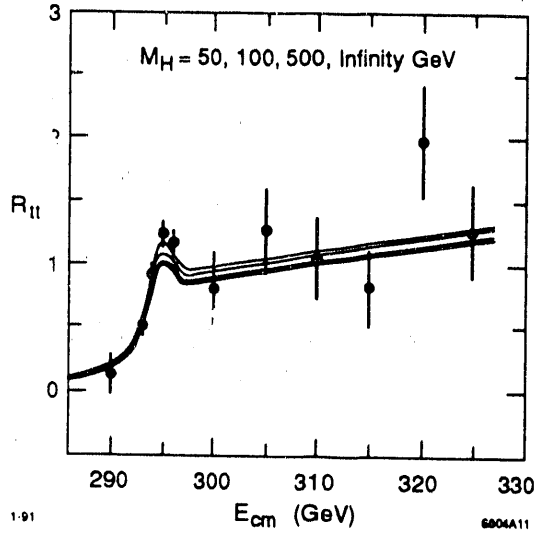

Fig. 11. In addition to the scan as shown in Fig. 8, more luminosity and energy points are added to try to see the minimal standard Higgs effect. The total integrated luminosity is 10 fb^{-1}.

C. *Higgs Boson Mass (M_H) and Higgs-top Coupling*

The Higgs boson coupling to a heavy fermion is as large as the Higgs gauge coupling to weak bosons. For a large mass top quark, the running α_s becomes smaller and the contribution of Higgs exchange in the $t\bar{t}$ bound state may become significant.

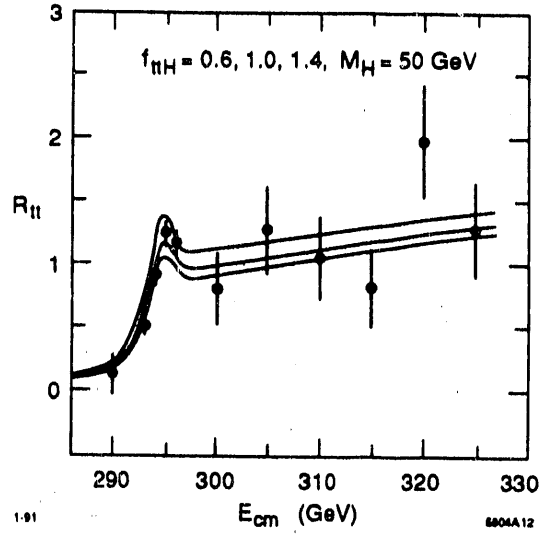

Fig. 12. In addition to the scan as shown in Fig. 8, more luminosity and energy points are added to measure the Higgs-top coupling (f_{ttH}) with an assumption that a 50 GeV Higgs boson would have been already found at LEP-II.

Since light Higgs bosons ($M_H \lesssim \sqrt{s}/2$) can be directly observed at the e^+e^- collider, we study whether heavier Higgs effects can be seen in the $t\bar{t}$ threshold region. The conclusion is that it is not possible to measure the Higgs mass in this way with the expected integrated luminosity Simultaneous fit of M_t and M_H for $M_t = 150$ GeV and $M_H = 200$ GeV assuming luminosity of 10 fb^{-1} in total (9 fb^{-1} is added to the basic scan at the sensitive energy points as shown in Fig. 11) we expect $\Delta M_t = 0.195$ GeV and $\Delta M_H = 191$ GeV.

Then the next question is how accurate we can measure the Higgs coupling to the top quark if a light Higgs boson has been found and if the Higgs mass has already been measured (Fig. 12). Assuming 100 GeV Higgs and a total luminosity of 10 fb^{-1} we expect $\Delta M_t = 0.188$ GeV and $\Delta f_{ttH} = 0.238$.

VI. CONCLUSION

The mass of a heavy top quark ($M_t \approx 125$–250 GeV) can be determined precisely by an energy scan near the $t\bar{t}$ threshold at e^+e^- colliders of $\sqrt{s} \approx 250$–500 GeV. Isolated leptons and spherical event shape can be used for selecting a clean $t\bar{t}$ sample. In the considered range of the top mass, the detection efficiency of >10% is obtained with the signal to background ratio of $\gtrsim 5 R_{t\bar{t}}$. With the total integrated luminosity of 1 fb^{-1}, the expected statistical error of 150 GeV top quark is ≈ 0.3 GeV. The resolution of the top mass measurement is considerably worse for the heavy top (1.0 GeV

for $M_t = 250$ GeV), if we measure with the same total luminosity. The systematic error in M_t due to the uncertainty in α_s is 0.3–0.5 GeV for $M_t = 150$ GeV, if the α_s can be measured at the Z peak with an accuracy of $\Delta\alpha_s = \pm 0.003$–$0.005$ and if there are no further theoretical ambiguities. Effects due to the unknown top quark decay width and Higgs mass effects are relatively small and are hard to measure with luminosity of about 1 fb^{-1}. The error correlations between M_t and Γ_t, and between M_t and M_H are small, and they do not affect the M_t measurement significantly. With larger integrated luminosity of $\gtrsim$10 fb^{-1}, it might be possible to determine Γ_t in an accuracy of $\mathcal{O}(10\%)$ and to determine the top-Higgs coupling to 25%, if the Higgs boson would have been found with the mass $\lesssim$50 GeV at LEP–II.

VII. ACKNOWLEDGEMENTS

I would like to thank M. Peskin and M. Strassler for providing me a user friendly computer program package to calculate the $t\bar{t}$ cross section taking into account the Higgs effects, and for useful discussions on the phenomenological aspects of top mass determination. I also would like to thank M. Swartz for useful discussions on the energy scan strategy.

REFERENCES

[1] M. L. Swartz, SLAC–PUB–5258.

[2] V. S. Fadin and V. A. Kohze, *JETP Lett.* **46**, 525 (1987).

[3] M. E. Peskin and M. J. Strassler, SLAC–PUB–5308.

[4] L. H. Orr and J. L. Rosner, *Phys. Lett.* **B246**, 221 (1990).

[5] T. Sjöstrand, *Comp. Phys. Comm.* **39**, 347 (1986); T. Sjöstrand and M. Bengtsson, *Comp. Phys. Comm.* **43**, 367 (1987).

[6] This Monte Carlo is based on M. Bohm et al., *Nucl. Phys.* **B304**, (1988) 463; A. Danner and T. Sack, *Nucl. Phys.* **B306**, 221 (1988).

[7] JADE Collab., W. Bartel et al., *Z. Physik,* **C33**, 29 (1986).

[8] This idea comes from M. E. Peskin. He wants experimentalists to study also purely hadronic modes, which I have not done for this workshop.

[9] Private communication, M. E. Peskin and M. J. Strassler.

[10] Mark II Collab., S. Komamiya et al., *Phys. Rev. Lett.* **64**, 987 (1990).

END

DATE FILMED

02 / 21 / 91